

Published in final edited form as:

*Vaccine*. 2012 June 6; 30(26): 3908–3917. doi:10.1016/j.vaccine.2012.03.079.

## High-efficiency Transduction of Human Monocyte-derived Dendritic Cells by Capsid-modified Recombinant AAV2 Vectors

George V. Aslanidi<sup>1,2,\*</sup>, Angela E. Rivers<sup>1</sup>, Luis Ortiz<sup>1</sup>, Lakshmanan Govindasamy<sup>3</sup>, Chen Ling<sup>1,2,4</sup>, Giridhara R. Jayandharan<sup>1,2,7</sup>, Sergei Zolotukhin<sup>1,2,4,5</sup>, Mavis Agbandje-McKenna<sup>2,3,5</sup>, and Arun Srivastava<sup>1,2,4,5,6,\*</sup>

<sup>1</sup>Division of Cellular and Molecular Therapy, Department of Pediatrics, University of Florida, College of Medicine, Gainesville, FL, USA

<sup>2</sup>Powell Gene Therapy Center, University of Florida, College of Medicine, Gainesville, FL, USA

<sup>3</sup>Department of Biochemistry & Molecular Biology, University of Florida, College of Medicine, Gainesville, FL, USA

<sup>4</sup>Department of Molecular Genetics & Microbiology, University of Florida, College of Medicine, Gainesville, FL, USA

<sup>5</sup>Genetics Institute, University of Florida, College of Medicine, Gainesville, FL, USA

<sup>6</sup>Shands Cancer Center, University of Florida, College of Medicine, Gainesville, FL, USA

<sup>7</sup>Department of Haematology and Centre for Stem Cell Research, Christian Medical College, Vellore, Tamil Nadu, India

### Abstract

Phosphorylation of surface-exposed tyrosine residues negatively impacts the transduction efficiency of recombinant AAV2 vectors. Pre-treatment of cells with specific cellular serine/threonine kinase inhibitors also significantly increased the transduction efficiency of AAV2 vectors. We reasoned that site-directed mutagenesis of surface-exposed serine residues might allow the vectors to evade phosphorylation and thus lead to higher transduction efficiency. Each of the 15 surface-exposed serine (S) residues was substituted with valine (V) residues, and the transduction efficiency of three of these mutants, S458V, S492V and S662V, was increased by up to ~20-fold in different cell types. The S662V mutant was efficient in transducing human monocyte-derived dendritic cells (moDCs), a cell type not readily amenable to transduction by the conventional AAV vectors, and did not induce any phenotypic changes in these cells. Recombinant S662V-AAV2 vectors encoding a truncated human telomerase (hTERT) gene were generated and used to stimulate cytotoxic T cells (CTLs) against target cells. S662V-AAV2-hTERT vector-transduced DCs resulted in rapid, specific T-cell clone proliferation and generation of robust CTLs, which led to specific cell lysis of K562 cells. These studies suggest that high-efficiency transduction of moDCs by serine-modified AAV2 vectors is feasible, which supports the potential utility of these vectors for future human DC vaccine studies.

© 2012 Elsevier Ltd. All rights reserved.

\*To whom correspondence and reprint requests should be addressed at the Division of Cellular and Molecular Therapy, Cancer and Genetics Research Complex, 2033 Mowry Road, Room 493, University of Florida College of Medicine, Gainesville, FL 32610, USA, Tel: 1-352-273-8258, Fax: 1-352-273-8342, aslanidi@peds.ufl.edu or aruns@peds.ufl.edu.

**Publisher's Disclaimer:** This is a PDF file of an unedited manuscript that has been accepted for publication. As a service to our customers we are providing this early version of the manuscript. The manuscript will undergo copyediting, typesetting, and review of the resulting proof before it is published in its final citable form. Please note that during the production process errors may be discovered which could affect the content, and all legal disclaimers that apply to the journal pertain.

## Keywords

adeno-associated virus vectors; capsid proteins; serine-phosphorylation; serine/threonine kinase; dendritic cells; gene expression

---

## Introduction

Dendritic cells (DCs) are antigen-presenting cells (APCs), which play a critical role in the regulation of the adaptive immune response. DCs are unique APCs and have been referred to as “professional” APCs, since the principal function of DCs is to present antigens, and because only DCs have the ability to induce a primary immune response in resting naïve T lymphocytes [1]. Although a naturally occurring anti-tumor immune response is detectable in patients, this response fails to control tumor growth. On the other hand, monocyte-derived DCs (moDCs) generated *ex vivo* in the presence of granulocyte-macrophage colony-stimulating factor (GM-CSF) and interleukin 4 (IL-4) possess the capacity to stimulate antigen-specific T-cells after endogenous expression of antigens [2, 3]. For this reason, genetically-modified DCs have been extensively studied and numerous Phase I and II clinical trials evaluating the efficacy of DCs in patients with cancer have been initiated [4, 5]. However, current methods for DC loading are inadequate in terms of cell viability, uncertainty regarding the longevity of antigen presentation, and the restriction by the patient's haplotype [5].

The possibility of manipulating viral genomes by biotechnological techniques, together with the recent identification of many tumor-associated antigens (TAAs), has sparked an interest in using recombinant viruses to express TAAs in the hope of inducing a protective antitumor immune response in patients [6, 7]. Among different methods for gene delivery, vectors based on a human parvovirus, the adeno-associated virus serotype 2 (AAV2), have attracted much attention mainly because of the non-pathogenic nature of this virus, and its ability to mediate long-term, sustained therapeutic gene expression [8-10]. Successful transduction of different subsets of DCs by different commonly used serotypes of AAV vectors has been demonstrated and the potential advantage of an AAV-based antitumor vaccine discussed [11-15]. However, further improvements in gene transfer by recombinant AAV vectors to DCs in terms of specificity and transduction efficiency are warranted to achieve a significant impact when used as an anti-tumor vaccine.

We have previously reported that the cellular epidermal growth factor receptor protein tyrosine kinase (EGFR-PTK) negatively impacts nuclear transport and subsequent transgene expression by recombinant AAV2 vectors primarily due to phosphorylation of capsids at surface tyrosine residues [16]. These studies resulted in the development of next generation recombinant AAV2 vectors containing point mutations in surface exposed tyrosine residues that transduce various cells and tissues with high-efficiency at lower doses compared to the wild-type (WT) vector [17]. However, such single or multiple tyrosine-mutant AAV vectors failed to increase the transduction efficiency of monocyte-derived DCs (moDCs) more than 2-fold, most likely due to lower levels of expression and/or activity of EGFR-PTK compared with that in HeLa cells or hepatocytes [15].

Serine/threonine protein kinases are involved in a wide variety of cellular processes such as differentiation, transcription regulation, and development of many cell types including immune cells. Such kinases can also negatively regulate the efficiency of recombinant AAV vector-mediated gene transfer by phosphorylating the surface-exposed serine and/or threonine residues on the viral capsid and target the vectors for proteasome-mediated degradation. We hypothesized that prevention of phosphorylation of the surface-exposed

serine residues might allow vectors to evade phosphorylation and subsequent ubiquitination and, thus, prevent proteasomal degradation. In the present studies, we document the following: (i) Site-directed mutagenesis of the 15 surface-exposed serine (S) residues on the AAV2 capsid to valine (V) residues leads to improved transduction efficiency of S458V, S492V, and S662V mutant vectors compared with the WT AAV2 vector; (ii) The S662V mutant vector efficiently transduces human monocyte-derived dendritic cells (moDCs), a cell type not readily amenable to transduction by the conventional AAV vectors; (iii) High-efficiency transduction of moDCs by S662V mutant does not induce any phenotypic changes in these cells; and (iv) Recombinant S662V- vectors encoding a truncated human telomerase (hTERT) gene, used to transduce DCs result in rapid, specific T-cell clone proliferation and generation of robust CTLs, which leads to specific cell lysis of K562 cells. These observations suggest that high-efficiency transduction of moDCs by serine-modified AAV2 vectors is feasible, which supports the potential utility of these vectors for future human DC vaccine studies.

## Results

### Inhibition of specific cellular serine/threonine kinase increases the transduction efficiency of recombinant AAV2 vectors

In our previous studies, we demonstrated that inhibition of cellular epidermal growth factor receptor protein tyrosine kinase (EGFR-PTK) activity, and site-directed mutagenesis of the 7 surface-exposed tyrosine residues significantly increases the transduction efficiency of AAV2 vectors by preventing phosphorylation of these residues, thereby circumventing ubiquitination and subsequent proteasome-mediated degradation of the vectors [18]. However, AAV2 capsids also contain 15 surface-exposed serine residues, which can potentially be phosphorylated by cellular serine/threonine kinases widely expressed in various cell types and tissues. To test our hypothesis that inhibition of such kinase activity can prevent phosphorylation of surface-exposed serine residues and thus improve intracellular trafficking and nuclear transport of AAV2 vectors, we used several commercially available specific inhibitors of cellular serine/threonine kinases, such as calmodulin-dependent protein kinase II (CamK-II), *c-Jun* N-terminal kinase (JNK); and mitogen-activated protein kinase (p38 MAPK). HEK293 cells were pre-treated with specific inhibitors, such as 2-(2-hydroxyethylamino)-6-aminohexylcarbamic acid *tert*-butyl ester-9-isopropylpurine (for CaMK-II), anthra[1,9-*cd*]pyrazol-6(2*H*)-one, 1,9-pyrazoloanthrone (for JNK), and 4-(4-fluorophenyl)-2-(4-methylsulfinylphenyl)-5-(4-pyridyl)1*H*-imidazole (for p38 MAPK) for 1 h at various concentrations. Cells were subsequently transduced with either single-stranded (ss) or self-complementary (sc) AAV2 vectors at 1,000 vector genomes (vgs) per cell. These results indicated that all inhibitors at an optimal concentration of 50  $\mu$ M significantly increased the transduction efficiency of both ssAAV2 and scAAV2 vectors, the p38 MAPK inhibitor being the most effective (Fig. 1a,b). This observation suggests, albeit does not prove, that the increase in the transduction efficiency was most likely due to prevention of phosphorylation of vector capsids rather than improved viral second-strand DNA synthesis.

### Site-directed mutagenesis of surface-exposed serine residues on AAV2 capsid improves AAV2 vector-mediated transgene expression

The AAV2 capsid contains 50 serine (S) residues in the viral protein 3 (VP3) common region of the three capsid VPs, of which 15 (S261, S264, S267, S276, S384, S458, S468, S492, S498, S578, S658, S662, S668, S707, S721) are surface-exposed [19]. Each of the 15 S residues was substituted with valine (V) by site-directed mutagenesis as described previously [17]. Most mutants could be generated at titers similar to the WT AAV2 vectors, with the exception of S261V, S276V, and S658V, which were produced at  $\sim$ 10 times lower

titers, and S267V and S668V, which produced no detectable levels of DNase I-resistant vector particles. The titers of S468V and S384V mutants were ~3-5 times higher than the WT AAV2 vectors. Each of the S-V mutant vectors was evaluated for transduction efficiency in HEK293 cells. These results, shown in Fig. 2, indicate that of the 15 mutants, the S662V mutant transduced HEK293 cells ~20-fold more efficiently than its WT counterpart. The transduction efficiency of the S458V and the S492V mutant vectors was increased by ~4- and 2-fold, respectively. The positions of these three critical surface exposed serine residues on the AAV2 capsid are shown in Fig. 3a,b. No further increase in transduction efficiency was observed with the double-mutants (S458+662V and S492+662V), or the triple-mutant (S458+492+662V), indicating that unlike some of the tyrosine-mutants [20], combining multiple mutations in the serine residues was neither additive nor synergistic. Interestingly, the transduction efficiency of the S468V and the S384V mutants, which were produced at titers higher than the WT AAV2 vectors, either remained unchanged (S468V), or was reduced ~10-fold (S384V) at the same multiplicity of infection (MOI). These data are summarized in the Table 1.

### **Substitution of the serine residue at position 662 with different amino acids has diverse effects on AAV2 capsid assembly as well as AAV2 vector-mediated transgene expression**

In addition to S-to-V substitution at position 662, we also generated the following 7 mutants with different amino acids: S662→Alanine (A), S662→Asparagine (N), S662→Aspartic acid (D), S662→Histidine (H), S662→Isoleucine (I), S662→Leucine (L), and S662→Phenylalanine (F), and evaluated their transduction efficiency in 293 cells. These results, shown in Fig. 4 and summarized in Table 2, demonstrate that the substitution of S with V led to the production of the most efficient mutant without any change in vector titers. Replacement of S with N, I, L, or F decreased the packaging efficiency ~10-fold with no significant effect on the transduction efficiency, whereas substitution with D or H increased the transduction efficiency ~8-fold and ~4-fold, respectively, with no effect on vector titers. Interestingly, substitution of S to A increased the viral titer up to ~5-fold, and enhanced the transgene expression ~3-fold compared with the WT AAV2 vector. The observed variability in titers and infectivity of the serine-mutants at position 662 suggests the critical role each of the amino acids plays in modulating both AAV2 packaging efficiency and biological activity.

### **Transduction efficiency of S662V vectors correlates with p38 MAPK activity in various cell types**

Since all of the S662V vector-mediated transgene expression data thus far were derived using 293 cells, we extended these studies to include the following cell types: (i) NIH3T3 (mouse embryonic fibroblasts), (ii) H2.35 (mouse fetal hepatocytes), (iii) HeLa (human cervical cancer cells), and (iv) primary human monocyte-derived dendritic cells (moDCs). These cell types were transduced with WT scAAV2-EGFP or S662V scAAV2-EGFP vectors at an MOI of 2,000 vgs per cell under identical conditions. EGFP gene expression was evaluated 48 hrs post-infection (p.i.) for HeLa, 293 and moDCs, and 5 days p.i. for H2.35 and NIH3T3 cells. These results are shown in Fig. 5a. As can be seen, although the absolute differences in the transduction efficiency between WT and S662V mutant vectors ranged from ~3-fold (in H2.35 cells) to ~20-fold (in 293 cells) the mutant vector was consistently more efficient in each cell type tested. Since pre-treatment of cells with an inhibitor of cellular p38 MAPK was the most effective in increasing the transduction efficiency (Fig. 1a,b), we wished to examine whether or not the observed differences in the transduction efficiency of the WT and the mutant vectors was due to variations in the levels of expression and/or activity of the cellular p38 MAPK. Cell lysates prepared from each cell type were analyzed on Western blots probed with specific antibodies to detect both total p38 MAPK and phospho-p38 MAPK levels. GAPDH was used as a loading control. These

results, shown in Fig. 5b, indicate that whereas the p38 MAPK protein levels were similar, the kinase activity, as determined by the level of phosphorylation, varied significantly among different cell types, and the transduction efficiency of the S662V mutant vector correlated roughly with the p38 MAPK activity. These approximate correlations between p38 MAPK activity and the efficiency of the S662V mutant vector can probably be explained by different cell susceptibilities for AAV infection, the overall number of viral particles entered cell after primary infection. It remains unclear as to which precise steps in the life cycle of AAV are modulated by p38 MAPK-mediated phosphorylation. It is also possible that other serine/threonine kinases contributing to the difference in efficiency of transduction by S662V and WT vectors. Interestingly, however, transduction by the WT-AAV2 vectors did not lead to up regulation of phosphorylation of p38 MAPK in 293 cells or in moDC (data not shown), further supporting a previous report that AAV does not induce robust phenotypic changes in moDCs [21].

### **S662V mutant vector-mediated transduction of primary human monocyte-derived dendritic cells (moDCs) does not lead to phenotypic alterations**

MAPK family members play important roles in the development and maturation of APCs. moDCs, isolated from healthy donor leukapheresis, were treated with 50  $\mu$ M selective kinase inhibitors as described above and then transduced with WT scAAV2-EGFP vectors. Two hrs p.i., cells were treated with supplements (TNF- $\alpha$ , IL-1 $\beta$ , 11-6, PGE2) to induce maturation. EGFP transgene expression was evaluated 48 hrs p.i. by fluorescence microscopy. Pre-treatment of moDCs with specific inhibitors of JNK and p38 MAPK increased EGFP expression levels  $\sim$ 2-fold and  $\sim$ 3-fold, respectively, and the transduction efficiency was enhanced by  $\sim$ 5-fold with the S662V mutant vectors (Fig. 6). Since inhibition of these kinases has previously been reported to prevent maturation of dendritic cells [22-24], we also evaluated the capability of S662V mutant to induce phenotypic changes in DCs. moDC were infected with an increasingly higher MOI up to 50,000 vgs per cell, harvested at 48 hrs p.i., and analyzed by fluorescence-activated cell sorting (FACS) for up regulation of surface co-stimulatory molecules. Flow cytometric analyses of DC maturation markers such as CD80, CD83 and CD86 indicated that, similar to WT AAV2 vectors, the S662V mutant vectors also did not induce the maturation of moDCs (Fig. 6c). This observation supports the previously described low immunogenicity of AAV vectors [14, 21].

### **Human telomerase (hTERT) specific cytotoxic T-lymphocyte (CTL) generation by moDC transduced with AAV2-S662V vectors**

Since the serine-mutant AAV2 vector-mediated transgene expression in moDC was significantly improved compared with the WT-AAV2 vectors, we evaluated the ability of S662V-loaded moDCs to stimulate the generation of cytotoxic T-lymphocytes and effective specific killing of the target cell. Given that human telomerase is recognized as a unique anti-cancer target [25, 26] commonly expressed in most cancer cells, we cloned a truncated human telomerase (hTERT) gene under the control of the chicken  $\beta$ -actin promoter and packaged the DNA into the AAV2 S662V mutant. Non-adherent peripheral blood mononuclear cells (PBMC) containing up to 25% of CD8 positive cells were stimulated once with moDC/hTERT delivered by the S662V vector. An immortalized myelogenous leukemia cell line, K562, was used for a two-color fluorescence assay of cell-mediated cytotoxicity to generate a killing curve with subsequently reduced effector to target cell ratio. Result of these experiments, shown in Fig. 7, suggest that moDC loaded with hTERT can effectively stimulate specific T cell clone proliferation and killing activity compared with moDC expressing GFP. Thus, since immunization strategies that generate rapid and potent effector responses are essential for effective immunotherapy, our results support the efficacy of AAV-based delivery methods for vaccination studies.

## Discussion

Although the possibility of genetically-modified dendritic cells stimulating a specific anti-tumor cytotoxic T cell response has been proven in a number of clinical trials, a reliable method for therapeutic antigen loading, control of expression, and antigen presentation has not yet been developed [27, 28]. Since the first attempts to transduce dendritic cells with conventional ssAAV vectors nearly a decade ago [11], significant progress has been made in increasing the transduction efficiency of these vectors. For example, the development of self-complementary AAV (scAAV) vectors has circumvented a major rate-limiting step of viral second-strand DNA synthesis which dramatically increases transgene expression levels in different subsets of dendritic cells [14, 29, 30]. AAV vector-based antigen delivery to dendritic cells has successfully been utilized for several cancer models [13, 31, 32].

The natural flexibility of AAV structural and regulatory viral components promotes rapid molecular evolution and formation of numerous serologically distinct serotypes [33-35]. Several studies have shown that one can take advantage of such plasticity of AAV to generate new vectors with different cell and tissue tropism [36, 37]. Other studies revealed that substitution of a single amino acid on the viral capsid can strongly affect viral titer, interaction with cellular receptor, tissue-tropism and trafficking from endosome to the nucleolus [18, 38]. Wu *et al.*, have reported that replacement of lysine to glutamine at position 531 (K531E) on AAV6 capsid reduces gene transfer to mouse hepatocytes *in vivo* and affinity for heparin. The reverse mutation (E531K) on AAV1 capsid increased liver transduction and imparted heparin binding [38]. Our recent data with AAV2 serotype vectors indicate that a single substitution of tyrosine to phenylalanine (Y→F) dramatically improves viral trafficking from endosome to the nucleolus by preventing capsid phosphorylation, subsequent ubiquitination and degradation via proteasome [17]. These studies have led to the generation of a number of vectors with increased transduction efficiency in different cell types and tissues. Such vectors were used to improve F.IX gene transfer to murine hepatocytes for the phenotypic correction of hemophilia B [20]. These tyrosine-mutant AAV vectors also led to high efficiency transduction of mouse retina for the potential treatment of ocular diseases [39]. Although AAV6 serotype has shown higher transduction efficiency than AAV2 in dendritic cells [12, 15], we have focused these studies on AAV2 because these vectors have been studied more extensively in both basic research and clinical settings, however in the future we plan to develop AAV6 vectors with similar strategy.

It has become abundantly clear that phosphorylation of surface-exposed tyrosine-residues on AAV2 capsids negatively impacts the transduction efficiency of these vectors, which can be dramatically augmented by the use of specific inhibitors of cellular EGFR-PTK, known to phosphorylate these residues [16]. In the present studies, we focused our efforts on delineating the role of phosphorylation of serine residues in the life cycle of AAV2 vectors.

Indeed, the transduction efficiency of both ssAAV and scAAV vectors could be augmented by pre-treatment of cells with specific inhibitors of JNK and p38 MAPK, implying that one or more surface-exposed serine and/threonine residues on the AAV2 capsid becomes phosphorylated inside the host cell and that this modification is detrimental to capsid trafficking to the nucleus.

Next, each of 15 surface-exposed serine residues was mutated individually, but only three of these mutations led to an increase in transduction efficiency in different cell types, which ranged from ~2-fold to ~20-fold. However, unlike the tyrosine-mutants [20], combining multiple mutations did not augment the transduction efficiency of either the double-mutants (S458+662V and S492+662V), or the triple-mutant (S458+492+662V) AAV2 vectors *in*

*vitro*. In this context, it is noteworthy that in a report by DiPrimio *et al.*, [40], in which the HI loop located between the H and I strands of the conserved core  $\beta$ -barrel and contains residue S662 was characterized, both site-directed mutagenesis and peptide substitutions showed that this capsid region plays a crucial role in AAV capsid assembly and viral genome packaging (Fig. 3a,b) [19]. Although the S662 residue was not specifically targeted in those studies, the transduction efficiency of most of these mutants was either unchanged, or was reduced by up to 27-fold. The HI loop, which forms interactions between icosahedral five-fold symmetry related VPs and lies on the floor of the depression surrounding this axis, was also proposed to undergo a conformational re-arrangement that opens up the channel located at the icosahedral fivefold axis following heparin binding by AAV2 [41]. Residues S458 and 492 are located adjacent to each other (contributed from symmetry related VPs) on the outer surface of the protrusions (surrounding the icosahedral three-fold axes) facing the depression at the two-fold axes (Fig. 3). Previous mutation of residues adjacent to S458A, S492A and S492T had no effect on capsid assembly and resulted in no effect on transduction efficiency [42], that is confirms our observation of the critical role which particular amino acids plays in packaging efficiency and biological activity of AAV. Additional structural analyses of our data for the observed low or no yield of some of the mutants revealed the following: For the three mutants with low yields, the side-chain of the residues interact with main-chain atoms from the same VP monomer, and S267V with a low titer, has an interaction with D269 from the same monomer. For another capsid mutant, S668V, which is located in the HI loop and shown to play a role in capsid assembly [40], no obvious disruption of interaction was observed with the substitution. Interestingly, all of these residues, regardless of assembly phenotype, are at interface positions but only 458 and 492 involved in inter-VP interactions. The other residues are only involved in intra-VP interactions, if any. Thus it is possible that the changes in the no capsid or low capsid yield mutants result in misfolding for their VPs or the abrogation of formation of multimers formation required for assembly when changed to alanine. These observation indicate that additional studies are warranted to gain a better understanding of the precise molecular mechanisms underlying the observed effects serine mutations on capsid assembly, and also in particular the increased transduction by the S458V, S492V, and S662V mutants.

In the setting of tumor immunotherapy, the time of T cell activation and the potency and longevity of CD8 T cell responses are crucial factors in determining therapeutic outcome. Thus, we also evaluated whether increased transduction efficiency of moDC by the serine-mutant AAV2 vectors correlated with superior priming of T cells. Human telomerase was used as a specific target since it has been shown in numerous studies and clinical trials to be an attractive candidate for a broadly expressed rejection antigen for many cancer patients [25, 26]. Our results suggest that modification of the AAV2 capsid might be beneficial in terms of producing more specific and effective vectors for gene delivery. It is also important that one of the main obstacles, the induction of immuno-competition in cellular immune responses against vector-derived and transgene-derived epitopes, can probably be overcome not only by the replication-deficiency and lack of viral proteins expressed by recombinant AAV2, but also the fact that less capsid of modified viral particles will be degraded by host proteosomes and thus, provide less material for presentation.

We were unable to unambiguously document whether the S662 residue, or any other surface-exposed S residue, was directly phosphorylated by the cellular JNK and/or p38 MAPK. However, the transduction efficiency of the S662V mutant vector was further augmented by pre-treatment of cells with specific inhibitors of JNK and p38 MAPK (data not shown), suggesting that one or more surface-exposed threonine (T) residues on AAV2 capsids are most likely phosphorylated by these kinases. The AAV2 capsid contains 17 surface-exposed threonine residues [19], and in our currently ongoing studies, we have begun to systematically mutate each of these T residues. We anticipate that the successful

completion of these studies will not only yield a much clearer overall picture of the role that capsid phosphorylation plays in the AAV life cycle, but the specific combination of tyrosine-, serine-, and threonine-mutations will lead to the generation of optimal AAV2 vectors for cell and gene therapy.

## Materials and Methods

### Cells and Antibodies

HEK293, HeLa and NIH3T3 cells were obtained from the American Type Culture Collection and maintained as monolayer cultures in DMEM (Invitrogen) supplemented with 10% FBS (Sigma) and antibiotics (Lonza). Leukapheresis-derived peripheral blood mononuclear cells (PBMCs) (AllCells) were purified on Ficoll-Paque (GEHealthCare), resuspended in serum-free AIM-V medium (Lonza), and semi-adherent cell fractions were incubated for 7 days with recombinant human IL-4 (500 U/mL) and GM-CSF (800 U/mL) (R&D Systems). Cell maturation was initiated with a cytokine mixture including 10 ng/mL TNF- $\alpha$ , 10 ng/mL IL-1, 10 ng/mL IL-6, and 1 mg/mL PGE2 (R&D Systems) for 48 hrs. Prior to EGFP expression cells were characterized for co-stimulatory molecules expression to ensure that they met the typical phenotype of mature dendritic cells (mDC) (CD80, RPE, murine IgG1; CD83, RPE, murine IgG1; CD86, FITC, murine IgG1; Invitrogen) [21].

### Site-directed mutagenesis

A two-stage PCR was performed with plasmid pACG2 as described previously [43] using Turbo *Pfu* Polymerase (Stratagen). Briefly, in stage one, two PCR extension reactions were performed in separate tubes for the forward and reverse PCR primer for 3 cycles. In stage two, the two reactions were mixed and a PCR reaction was performed for an additional 15 cycles, followed by Dpn I digestion for 1 hr. Primers were designed to introduce changes from serine (*TCA* or *AGC*) to valine (*GTA* or *GTC*) for each of the residues mutated.

### Production of recombinant AAV vectors

Recombinant AAV2 vectors containing the EGFP gene driven by the chicken  $\beta$ -actin promoter were generated as described previously [44]. Briefly, HEK293 cells were transfected using Polyethelenimine (PEI, linear, MW 25,000, Polysciences, Inc.). Seventy-two hrs post transfection, cells were harvested and vectors were purified by iodixanol (Sigma) gradient centrifugation and ion exchange column chromatography (HiTrap Sp Hp 5 ml, GE Healthcare). Virus was then concentrated and the buffer exchanged in three cycles to lactated Ringer's using centrifugal spin concentrators (Apollo, 150-kDa cut-off, 20-ml capacity, CLP) [45]. Ten  $\mu$ l of purified virus was treated with DNase I (Invitrogen) for 2 hrs at 37°C, then an additional 2 hrs with proteinase K (Invitrogen) at 56°C. The reaction mixture was purified by phenol/chloroform, followed by chloroform treatment. Packaged DNA was precipitated with ethanol in the presence of 20  $\mu$ g glycogen (Invitrogen). DNase I-resistant AAV particle titers were determined by RT-PCR with the following primer-pair, specific for the CBA promoter: forward 5'-TCCCATAGTAACGCCAATAGG-3', reverse 5'-CTTGTCATATGATACACTTGATG-3' and SYBR Green PCR Master Mix (Invitrogen) [46].

### Recombinant AAV Vector Transduction Assays In Vitro

HEK293 or monocyte-derived dendritic cells (moDCs), were transduced with AAV2 vectors with 1,000 vgs/cell or 2,000 vgs/cell respectively, and incubated for 48 hrs. Alternatively, cells were pretreated with 50  $\mu$ M of selective serine/threonine kinase inhibitors 2-(2-hydroxyethylamino)-6-aminoethylcarbamic acid *tert*-butyl ester-9-isopropylpurine (for CaMK-II), anthra[1,9-*cd*]pyrazol-6(2*H*)-one, 1,9-pyrazoloanthrone (for JNK), and 4-(4-

fluorophenyl)-2-(4-methylsulfinylphenyl)-5-(4-pyridyl)1H-imidazole (for MAPK) (CK59, JNK inhibitor 2, PD 98059, Calbiochem), 1 hr before transduction. Transgene expression was assessed as the total area of green fluorescence (pixel<sup>2</sup>) per visual field (mean ± SD) as described previously [20, 21]. Analysis of variance was used to compare test results and the control, which were determined to be statistically significant.

### Western Blot Analysis

Western blot analysis was performed as described previously [47]. Cells were harvested by centrifugation, washed with PBS, and resuspended in lysis buffer containing 50 mM Tris\_HCl, pH 7.5, 120 mM NaCl, 1% Nonidet P-40, 10% glycerol, 10 mM Na<sub>4</sub>P<sub>2</sub>O<sub>7</sub>, 1 mM phenylmethylsulfonyl fluoride (PMSF), 1 mM EDTA, and 1 mM EGTA supplemented with protease and phosphatase inhibitors mixture (Set 2 and 3, Calbiochem). The suspension was incubated on ice for 1 hr and clarified by centrifugation for 30 min at 14,000 rpm at 4°C. Following normalization for protein concentration, samples were separated using 12% polyacrylamide/SDS electrophoresis, transferred to a nitrocellulose membrane, and probed with primary antibodies, anti p-p38 MAPK (Thr180/Tyr182) rabbit mAb, total p38 MAPK rabbit mAb and GAPDH rabbit mAb (1:1000, CellSignaling), followed by secondary horseradish peroxidase-linked antibodies (1:1000, CellSignaling).

### Specific cytotoxic T-lymphocytes generation and cytotoxicity assay

Monocyte-derived dendritic cells (moDCs) were generated as described above. Immature DCs were infected with AAV2-S662V vectors encoding human telomerase cDNA (a generous gift from Dr. Karina Krotova, University of Florida), separated into two overlapping ORF – hTERT<sub>838-2229</sub> and hTERT<sub>2042-3454</sub> at MOI 2,000 vgs/cell of each. Cells were then allowed to undergo stimulation with supplements to induce maturation. After 48 hrs, the mature DCs expressing hTERT were harvested and mixed with the PBMCs at a ratio of 20:1. CTLs were cultured in AIM-V medium containing recombinant human IL-15 (20 IU/ml) and IL-7 (20 ng/ml) at 20×10<sup>6</sup> cells in 25 cm<sup>2</sup> flasks. Fresh cytokines were added every 2 days. After 7 days post-priming, the cells were harvested and used for killing assays [48]. A killing curve was generated and specific cell lysis was determined by FACS analysis of live/dead cell ratios as described previously [49]. Human immortalized myelogenous leukemia cell line, K562, was used as a target.

### Statistical analysis

Results are presented as mean ± S.D. Differences between groups were identified using a grouped-unpaired two-tailed distribution of Student's T-test. P-values <0.05 were considered statistically significant.

### Acknowledgments

We thank Drs. Kenneth I. Berns and Nicholas Muzyczka for a critical reading of this manuscript. We thank Robery Ng for assistance in the preparation of Figure 3. This research was supported in part by a Junior Investigator Award from the University of Florida Shands Cancer Center, American Cancer Society Chris DiMarco Institutional Research Grant (to GVA), and Public Health Service grants P01 DK-058327 - Project 1 (to AS), R01 HL-097088 (to AS and SZ), and R01 GM-082946 (to SZ and MA-M) from the National Institutes of Health. GRJ was supported in part by an 'Overseas Associate Fellowship-2006' from the Department of Biotechnology, Government of India.

### References

1. Banchereau J, Steinman RM. Dendritic cells and the control of immunity. *Nature*. 1998 Mar 19; 392(6673):245–52. [PubMed: 9521319]

2. Chapuis F, Rosenzweig M, Yagello M, Ekman M, Biberfeld P, Gluckman JC. Differentiation of human dendritic cells from monocytes in vitro. *Eur J Immunol*. 1997 Feb; 27(2):431–41. [PubMed: 9045914]
3. den Brok MH, Nierkens S, Figdor CG, Ruers TJ, Adema GJ. Dendritic cells: tools and targets for antitumor vaccination. *Expert Rev Vaccines*. 2005 Oct; 4(5):699–710. [PubMed: 16221071]
4. Figdor CG, de Vries IJ, Lesterhuis WJ, Melief CJ. Dendritic cell immunotherapy: mapping the way. *Nat Med*. 2004 May; 10(5):475–80. [PubMed: 15122249]
5. Palucka K, Ueno H, Banchereau J. Recent Developments in Cancer Vaccines. *The Journal of Immunology*. Feb 1; 2011 186(3):1325–31. [PubMed: 21248270]
6. Liu MA. Immunologic basis of vaccine vectors. *Immunity*. 2010 Oct 29; 33(4):504–15. [PubMed: 21029961]
7. Robert-Guroff M. Replicating and non-replicating viral vectors for vaccine development. *Curr Opin Biotechnol*. 2007 Dec; 18(6):546–56. [PubMed: 18063357]
8. Daya S, Berns KI. Gene therapy using adeno-associated virus vectors. *Clin Microbiol Rev*. 2008 Oct; 21(4):583–93. [PubMed: 18854481]
9. Mueller C, Flotte TR. Clinical gene therapy using recombinant adeno-associated virus vectors. *Gene therapy*. 2008 Jun; 15(11):858–63. [PubMed: 18418415]
10. Srivastava A. Adeno-associated virus-mediated gene transfer. *J Cell Biochem*. 2008 Sep 1; 105(1):17–24. [PubMed: 18500727]
11. Ponnazhagan S, Mahendra G, Curiel DT, Shaw DR. Adeno-Associated Virus Type 2-Mediated Transduction of Human Monocyte-Derived Dendritic Cells: Implications for Ex Vivo Immunotherapy. *J Virol*. Oct 1; 2001 75(19):9493–501. [PubMed: 11533211]
12. Veron P, Allo V, Riviere C, Bernard J, Douar AM, Masurier C. Major Subsets of Human Dendritic Cells Are Efficiently Transduced by Self-Complementary Adeno-Associated Virus Vectors 1 and 2. *J Virol*. May 15; 2007 81(10):5385–94. [PubMed: 17314166]
13. Mahadevan M, Liu Y, You C, Luo R, You H, Mehta JL, et al. Generation of robust cytotoxic T lymphocytes against prostate specific antigen by transduction of dendritic cells using protein and recombinant adeno-associated virus. *Cancer Immunol Immunother*. 2007 Oct; 56(10):1615–24. [PubMed: 17356843]
14. Shin O, Kim SJ, Lee WI, Kim JY, Lee H. Effective transduction by self-complementary adeno-associated viruses of human dendritic cells with no alteration of their natural characteristics. *J Gene Med*. 2008 Jul; 10(7):762–9. [PubMed: 18452239]
15. Ussher JE, Taylor JA. Optimized transduction of human monocyte-derived dendritic cells by recombinant adeno-associated virus serotype 6. *Hum Gene Ther*. 2010 Dec; 21(12):1675–86. [PubMed: 20578847]
16. Zhong L, Zhao W, Wu J, Li B, Zolotukhin S, Govindasamy L, et al. A dual role of EGFR protein tyrosine kinase signaling in ubiquitination of AAV2 capsids and viral second-strand DNA synthesis. *Mol Ther*. 2007 Jul; 15(7):1323–30. [PubMed: 17440440]
17. Zhong L, Li B, Mah CS, Govindasamy L, Agbandje-McKenna M, Cooper M, et al. Next generation of adeno-associated virus 2 vectors: Point mutations in tyrosines lead to high-efficiency transduction at lower doses. *Proceedings of the National Academy of Sciences*. Jun 3; 2008 105(22):7827–32.
18. Zhong L, Li B, Jayandharan G, Mah CS, Govindasamy L, Agbandje-McKenna M, et al. Tyrosine-phosphorylation of AAV2 vectors and its consequences on viral intracellular trafficking and transgene expression. *Virology*. 2008 Nov 25; 381(2):194–202. [PubMed: 18834608]
19. Xie Q, Bu W, Bhatia S, Hare J, Somasundaram T, Azzi A, et al. The atomic structure of adeno-associated virus (AAV-2), a vector for human gene therapy. *Proc Natl Acad Sci U S A*. 2002 Aug 6; 99(16):10405–10. [PubMed: 12136130]
20. Markusic DM, Herzog RW, Aslanidi GV, Hoffman BE, Li B, Li M, et al. High-efficiency transduction and correction of murine hemophilia B using AAV2 vectors devoid of multiple surface-exposed tyrosines. *Mol Ther*. 2011 Dec; 18(12):2048–56. [PubMed: 20736929]
21. Jayandharan GR, Aslanidi G, Martino AT, Jahn SC, Perrin GQ, Herzog RW, et al. Activation of the NF- $\kappa$ B pathway by adeno-associated virus (AAV) vectors and its implications in immune

- response and gene therapy. *Proceedings of the National Academy of Sciences*. Mar 1; 2011 108(9):3743–8.
22. Boislevé F, Kerdine-Romer S, Pallardy M. Implication of the MAPK pathways in the maturation of human dendritic cells induced by nickel and TNF- $\alpha$ . *Toxicology*. 2005 Jan 15; 206(2):233–44. [PubMed: 15588916]
  23. Nakahara T, Moroi Y, Uchi H, Furue M. Differential role of MAPK signaling in human dendritic cell maturation and Th1/Th2 engagement. *J Dermatol Sci*. 2006 Apr; 42(1):1–11. [PubMed: 16352421]
  24. Nakahara T, Uchi H, Urabe K, Chen Q, Furue M, Moroi Y. Role of c-Jun N-terminal kinase on lipopolysaccharide induced maturation of human monocyte-derived dendritic cells. *Int Immunol*. 2004 Dec; 16(12):1701–9. [PubMed: 15477228]
  25. Harley CB. Telomerase and cancer therapeutics. *Nat Rev Cancer*. 2008 Mar; 8(3):167–79. [PubMed: 18256617]
  26. Beatty GL, Vonderheide RH. Telomerase as a universal tumor antigen for cancer vaccines. *Expert Rev Vaccines*. 2008 Sep; 7(7):881–7. [PubMed: 18767939]
  27. O'Neill DW, Bhardwaj N. Exploiting dendritic cells for active immunotherapy of cancer and chronic infections. *Mol Biotechnol*. 2007 Jun; 36(2):131–41. [PubMed: 17914192]
  28. Tacken PJ, de Vries IJ, Torensma R, Figdor CG. Dendritic-cell immunotherapy: from ex vivo loading to in vivo targeting. *Nat Rev Immunol*. 2007 Oct; 7(10):790–802. [PubMed: 17853902]
  29. Aldrich WA, Ren C, White AF, Zhou SZ, Kumar S, Jenkins CB, et al. Enhanced transduction of mouse bone marrow-derived dendritic cells by repetitive infection with self-complementary adeno-associated virus 6 combined with immunostimulatory ligands. *Gene therapy*. 2006 Jan; 13(1):29–39. [PubMed: 16136165]
  30. Wang Z, Ma HI, Li J, Sun L, Zhang J, Xiao X. Rapid and highly efficient transduction by double-stranded adeno-associated virus vectors in vitro and in vivo. *Gene therapy*. 2003 Dec; 10(26):2105–11. [PubMed: 14625564]
  31. Eisold S, Schmidt J, Ryschich E, Gock M, Klar E, von Knebel Doeberitz M, et al. Induction of an antitumoral immune response by wild-type adeno-associated virus type 2 in an in vivo model of pancreatic carcinoma. *Pancreas*. 2007 Jul; 35(1):63–72. [PubMed: 17575547]
  32. Yu Y, Pilgrim P, Zhou W, Gagliano N, Frezza EE, Jenkins M, et al. rAAV/Her-2/neu loading of dendritic cells for a potent cellular-mediated MHC class I restricted immune response against ovarian cancer. *Viral Immunol*. 2008 Dec; 21(4):435–42. [PubMed: 19115932]
  33. Gao G, Alvira MR, Somanathan S, Lu Y, Vandenberghe LH, Rux JJ, et al. Adeno-associated viruses undergo substantial evolution in primates during natural infections. *Proc Natl Acad Sci U S A*. 2003 May 13; 100(10):6081–6. [PubMed: 12716974]
  34. Vandenberghe LH, Wilson JM, Gao G. Tailoring the AAV vector capsid for gene therapy. *Gene therapy*. 2009 Mar; 16(3):311–9. [PubMed: 19052631]
  35. Wu Z, Asokan A, Samulski RJ. Adeno-associated virus serotypes: vector toolkit for human gene therapy. *Mol Ther*. 2006 Sep; 14(3):316–27. [PubMed: 16824801]
  36. Wu P, Xiao W, Conlon T, Hughes J, Agbandje-McKenna M, Ferkol T, et al. Mutational analysis of the adeno-associated virus type 2 (AAV2) capsid gene and construction of AAV2 vectors with altered tropism. *Journal of virology*. 2000 Sep; 74(18):8635–47. [PubMed: 10954565]
  37. Girod A, Ried M, Wobus C, Lahm H, Leike K, Kleinschmidt J, et al. Genetic capsid modifications allow efficient re-targeting of adeno-associated virus type 2. *Nat Med*. 1999 Dec; 5(12):1438. [PubMed: 10581091]
  38. Wu Z, Asokan A, Grieger JC, Govindasamy L, Agbandje-McKenna M, Samulski RJ. Single amino acid changes can influence titer, heparin binding, and tissue tropism in different adeno-associated virus serotypes. *Journal of virology*. 2006 Nov; 80(22):11393–7. [PubMed: 16943302]
  39. Petrs-Silva H, Dinculescu A, Li Q, Min SH, Chiodo V, Pang JJ, et al. High-efficiency transduction of the mouse retina by tyrosine-mutant AAV serotype vectors. *Mol Ther*. 2009 Mar; 17(3):463–71. [PubMed: 19066593]
  40. DiPrimio N, Asokan A, Govindasamy L, Agbandje-McKenna M, Samulski RJ. Surface Loop Dynamics in Adeno-Associated Virus Capsid Assembly. *J Virol*. Jun 1; 2008 82(11):5178–89. [PubMed: 18367523]

41. Levy HC, Bowman VD, Govindasamy L, McKenna R, Nash K, Warrington K, et al. Heparin binding induces conformational changes in Adeno-associated virus serotype 2. *J Struct Biol.* 2009 Mar; 165(3):146–56. [PubMed: 19121398]
42. Lochrie MA, Tatsuno GP, Christie B, McDonnell JW, Zhou S, Surosky R, et al. Mutations on the external surfaces of adeno-associated virus type 2 capsids that affect transduction and neutralization. *Journal of virology.* 2006 Jan; 80(2):821–34. [PubMed: 16378984]
43. Wang W, Malcolm BA. Two-stage PCR protocol allowing introduction of multiple mutations, deletions and insertions using QuikChange Site-Directed Mutagenesis. *Biotechniques.* 1999 Apr; 26(4):680–2. [PubMed: 10343905]
44. Zolotukhin S, Potter M, Zolotukhin I, Sakai Y, Loiler S, Fraites TJ Jr, et al. Production and purification of serotype 1, 2, and 5 recombinant adeno-associated viral vectors. *Methods.* 2002 Oct; 28(2):158–67. [PubMed: 12413414]
45. Cheng B, Ling C, Dai Y, Lu Y, Glushakova LG, Gee SW, et al. Development of optimized AAV3 serotype vectors: mechanism of high-efficiency transduction of human liver cancer cells. *Gene therapy.* 2011 Jul 21.
46. Aslanidi G, Lamb K, Zolotukhin S. An inducible system for highly efficient production of recombinant adeno-associated virus (rAAV) vectors in insect Sf9 cells. *Proceedings of the National Academy of Sciences.* Mar 31; 2009 106(13):5059–64.
47. Aslanidi G, Kroutov V, Philipsberg G, Lamb K, Campbell-Thompson M, Walter GA, et al. Ectopic expression of Wnt10b decreases adiposity and improves glucose homeostasis in obese rats. *American Journal of Physiology - Endocrinology And Metabolism.* Sep 1; 2007 293(3):E726–E36. [PubMed: 17578883]
48. Heiser A, Coleman D, Dannull J, Yancey D, Maurice MA, Lallas CD, et al. Autologous dendritic cells transfected with prostate-specific antigen RNA stimulate CTL responses against metastatic prostate tumors. *J Clin Invest.* 2002 Feb; 109(3):409–17. [PubMed: 11828001]
49. Mattis AE, Bernhardt G, Lipp M, Forster R. Analyzing cytotoxic T lymphocyte activity: a simple and reliable flow cytometry-based assay. *J Immunol Methods.* 1997 May 26; 204(2):135–42. [PubMed: 9212830]

### Highlights

- Inhibition of p38 MAPK increases transduction efficiency of moDC by AAV2 vectors
- Mutagenesis of serine residues increases transduction efficiency of moDC by AAV2
- Transduction of moDC by mutant AAV2 does not induce phenotypic changes in these cells
- DC transduced with mutant AAV2 encoding a human telomerase stimulates specific CTLs

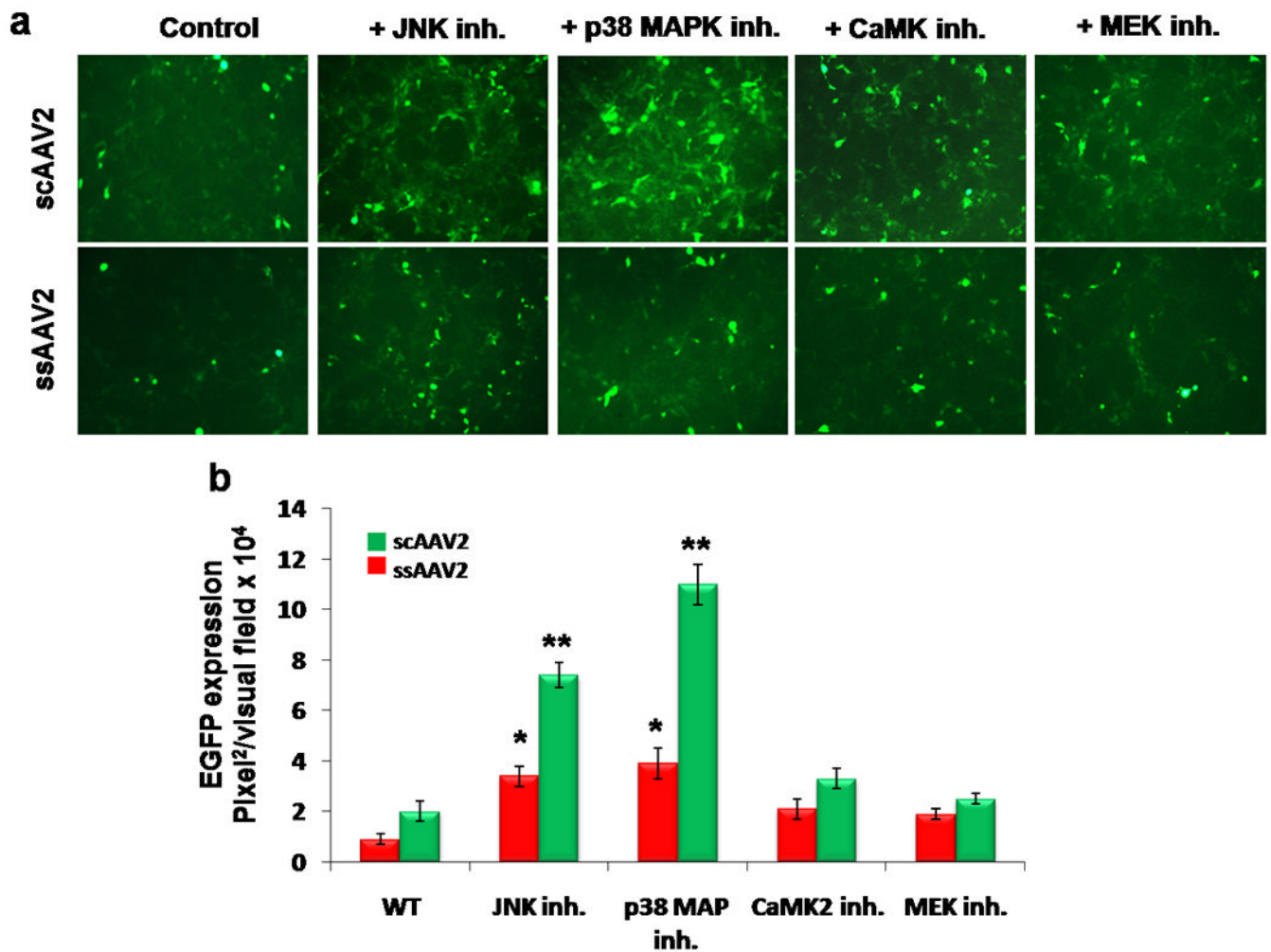


**Fig. 1.** Effect of various kinase inhibitors on ssAAV and scAAV mediated EGFP expression in HEK293 cells. Cells were pretreated with inhibitors for 1 hr before infection then transduced with  $1 \times 10^3$  vgs/cell. **(a)** Transgene expression was detected by fluorescence microscopy 48 hrs post infection. **(b)** Images from three visual fields were analyzed as described in *Materials and Methods*. \* $P < 0.005$ , \*\* $P < 0.001$  vs. WT AAV2.

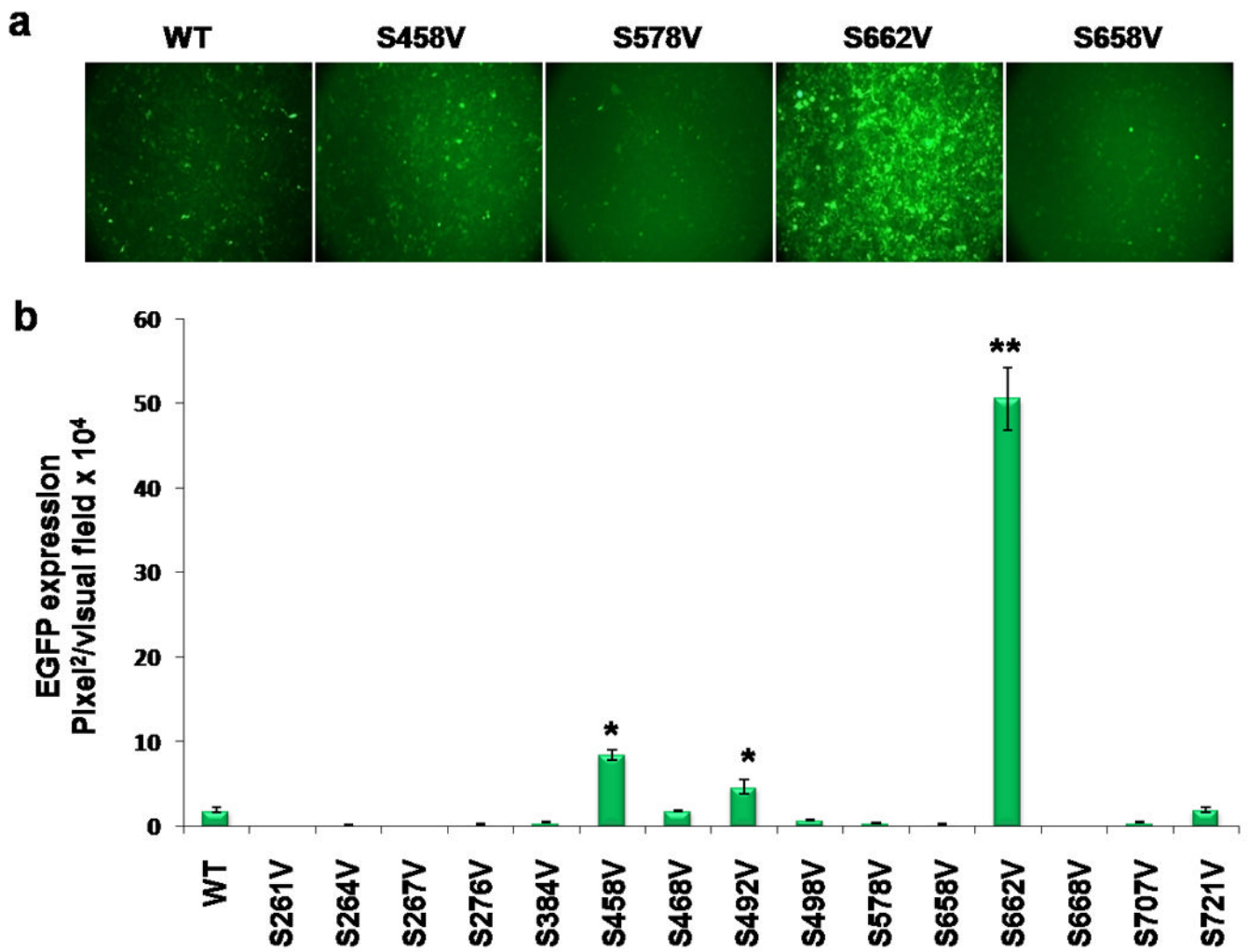


**Fig. 2.** Analysis of EGFP expression after transduction of HEK293 cells with individual site-directed scAAV2 capsid mutants. Each of the 15 surface-exposed serines (S) in AAV2 capsid was substituted with valine (V) and evaluated for its efficiency to mediate transgene expression. **(a)** EGFP expression analysis at 48 hrs post-infection at an MOI of  $1 \times 10^3$  vgs/cell. **(b)** Quantitation of transduction efficiency of each of the serine-mutant AAV2 vectors. \* $P < 0.005$ , \*\* $P < 0.001$  vs. WT AAV2.

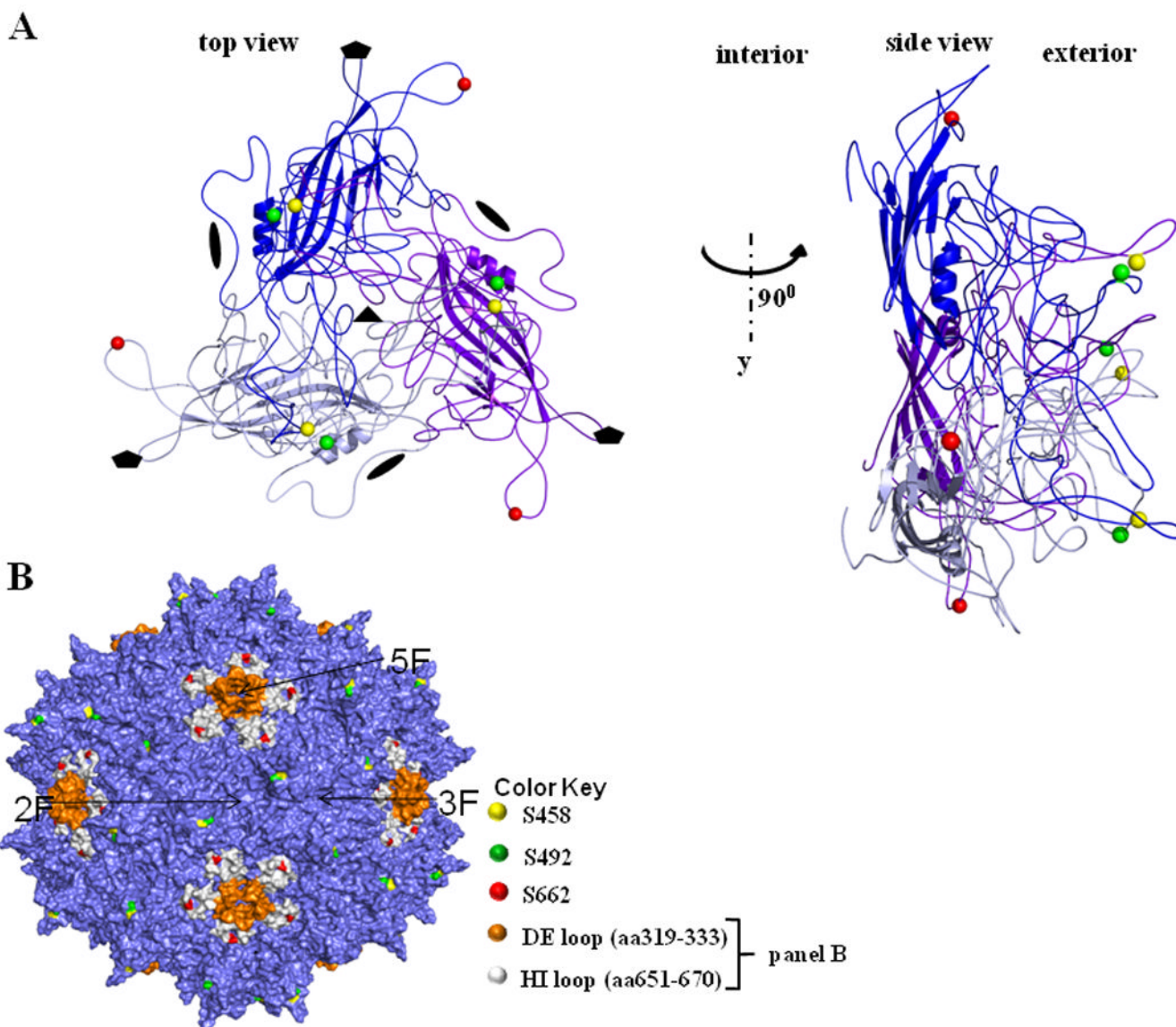


**Fig. 3.** The AAV2 structure. (A) A trimer of the AAV2 VP3 shown in ribbon representation and viewed down the icosahedral threefold axis (left) and rotated 90° (right) with VP monomers colored in blue, purple and light blue showing the location of serine residues 458, 492, and 662 in the yellow, green, and red spheres, respectively. The approximate positions of the icosahedral two-, three-, and five-fold axes are depicted by the filled oval, triangle, and pentagon, respectively. (B) The capsid surface of AAV2 shown in blue with serine residues 458, 492, and 662 highlighted in the same colors as in (A). S458 and 492 are located adjacent to each other on the outer surface of the protrusions facing the depression surrounding the two-fold axes. S662 is located on the HI loop (colored white) (between the  $\beta$ -H and  $\beta$ -I strands of the core eight-stranded beta-barrel) which lie on the floor of the depression surrounding the icosahedral five-fold axes. The five-fold symmetry related DE loops (between the  $\beta$ -D and  $\beta$ -E strands), which form the channel at the icosahedral 5-fold axes, are colored in brown. The approximate positions of an icosahedral two-fold (2F), three-fold (3F), and five-fold (5F) axes are indicated by the open arrows.

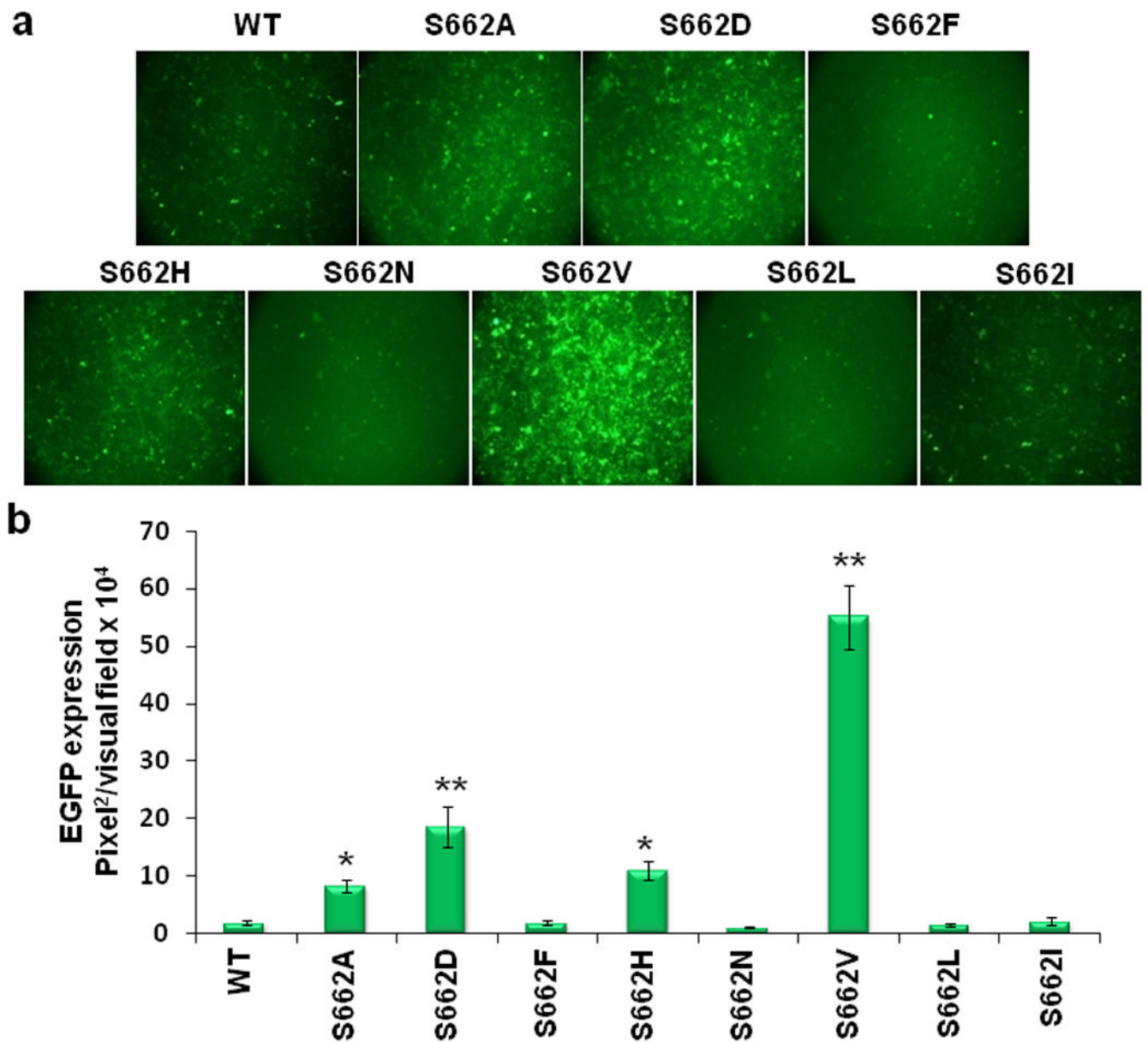


**Fig. 4.** Evaluation of the effect of serine substitution at position 662 in the scAAV2 capsid with different amino acids in mediating transgene expression. The following 8 serine mutants were generated with different amino acids: S662→Valine (V), S662→Alanine (A), S662→Asparagine (N), S662→Aspartic acid (D), S662→Histidine (H), S662→Isoleucine (I), S662→Leucine (L), and S662→Phenylalanine (F), and their transduction efficiency in 293 cells was analyzed. **(a)** EGFP expression analysis at 48 h after infection of 293 cells at an MOI of  $1 \times 10^3$  vgs/cell. **(b)** Quantitation of the transduction efficiency of each of the serine-mutant AAV2 vectors. \* $P < 0.005$ , \*\* $P < 0.001$  vs. WT AAV2.

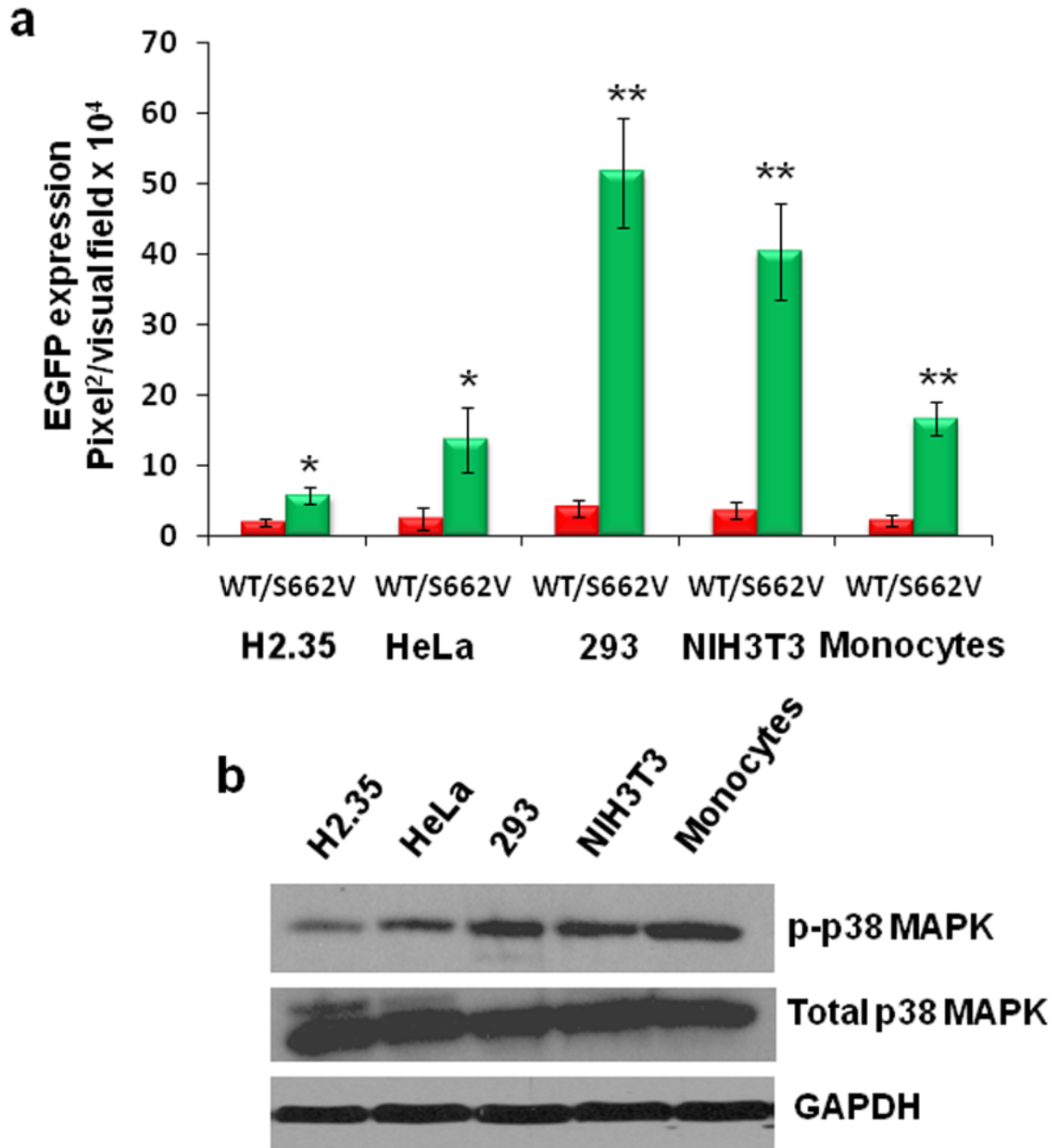


**Fig. 5.** Analysis of correlation of transduction efficiency of scAAV2-S662V vectors with p38 MAPK activity in various cell types. **(a)** Quantitation of the transduction efficiency of WT- and S662V-AAV2 vectors in HEK293, HeLa, NIH3T3, H2.35 and moDCs. **(b)** Western blot analysis of lysates from different cell lines for p-p38 MAPK expression levels. Total p38 MAPK and GAPDH levels were measured and used as loading controls. \* $P < 0.005$ , \*\* $P < 0.001$  vs. WT AAV2.

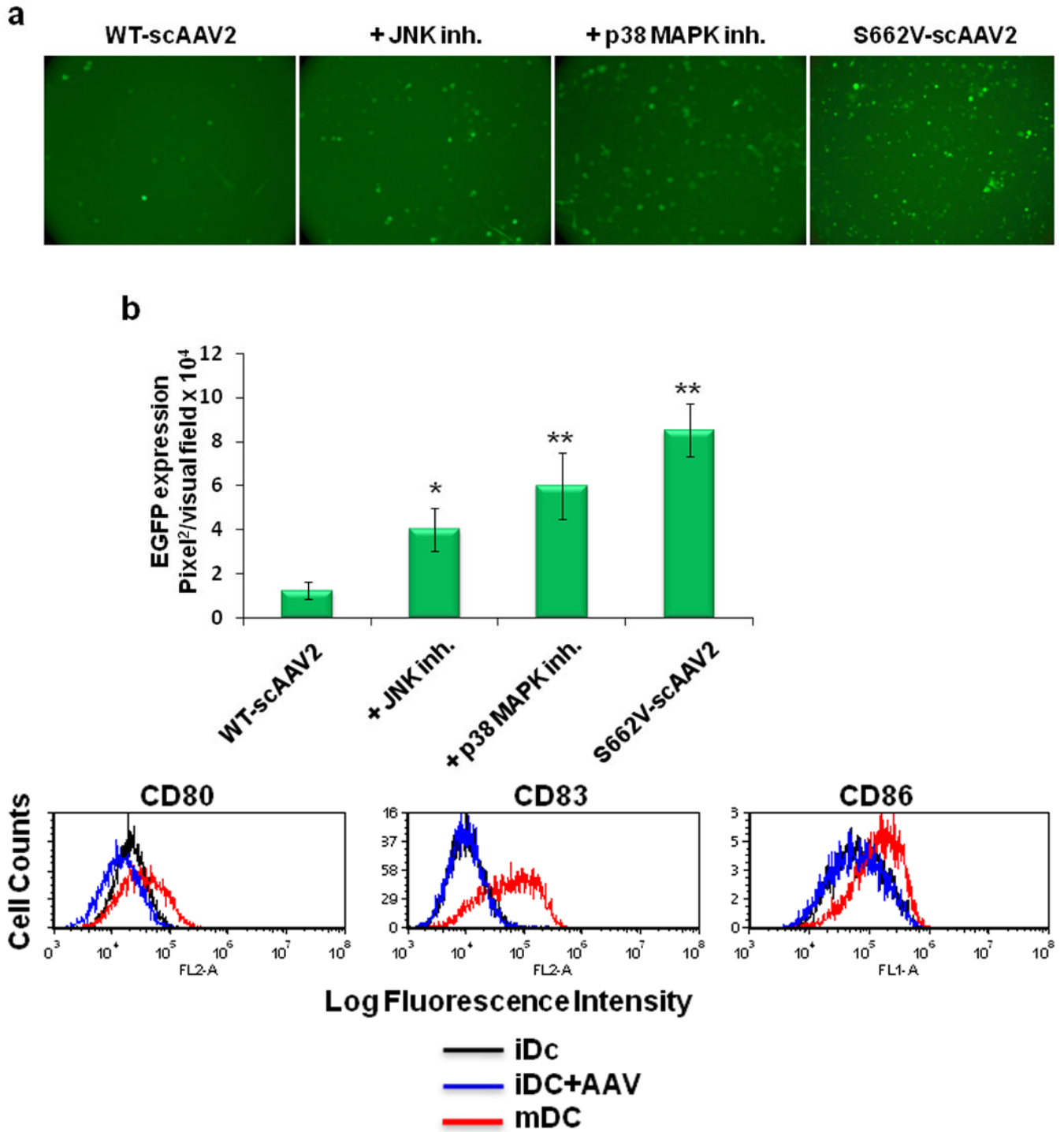


**Fig. 6.** scAAV vector-mediated transgene expression in monocyte-derived dendritic cells (moDCs). **(a)** Effect of JNK and p38 MAPK inhibitors, and site-directed substitution of the serine residue at position 662 on EGFP expression. **(b)** Quantitation of the data in **(a)** at 48 hrs after infection and initiation of maturation. **(c)** Analysis of expression of co-stimulatory markers such as CD80, CD83, CD86 in moDCs infected with scAAV2-S662V vectors at an

MOI of  $5 \times 10^4$  vgs/cell. iDCs – immature dendritic cells, and mDCs – mature dendritic cells, stimulated with cytokines, generated as described in *Materials and Methods*, were used as negative and positive controls, respectively. A representative example is shown. \* $P < 0.005$ , \*\* $P < 0.001$  vs. WT AAV2.

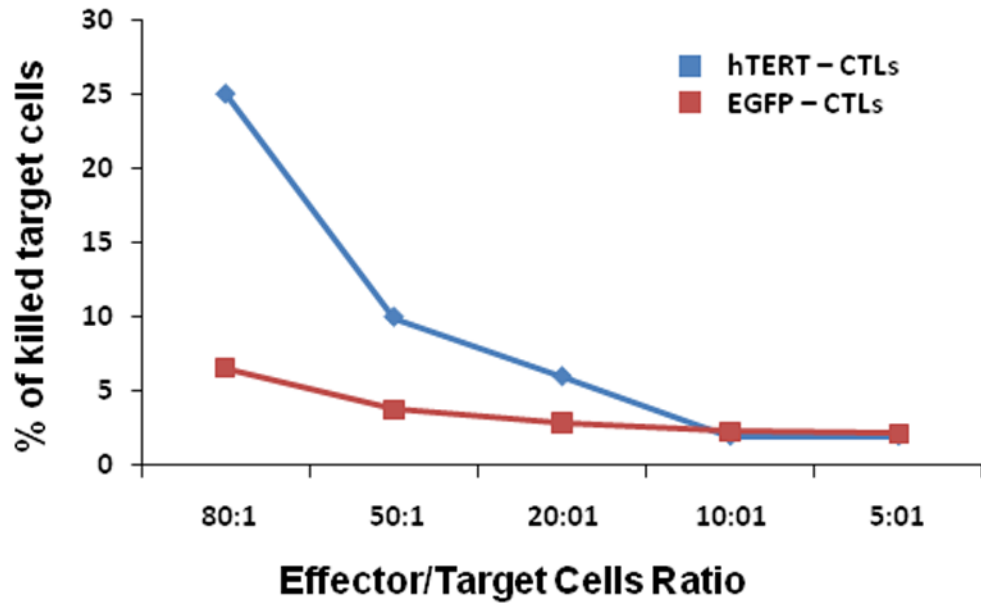


**Fig. 7.**

Analysis of hTERT-specific cytotoxic T-lymphocytes (CTLs) killing activity on K562 cells. CTLs were generated after transduction of moDCs by scAAV2-S662V vectors encoding the truncated human telomerase (hTERT). scAAV2-S662V-EGFP vector-transduced moDCs were used to generate non-specific CTLs. Pre-stained with 3,3-dioctadecyloxacarbocyanine (DiOC18(3)), a green fluorescent membrane stain,  $1 \times 10^5$  target K562 cells were co-cultured overnight with different ratios of CTLs (80:1, 50:1, 20:1, 10:1, 5:1). Membrane-permeable nucleic acid counter-stain, propidium iodide, was added to label the cells with compromised plasma membranes. Percentages of killed, double stain-positive cells were analyzed by flow cytometry.

**Table 1**  
**Packaging and transduction efficiencies of various serine-valine mutant AAV2 vectors relative to WT AAV2 vectors**

Mutant	Packaging Efficiency	Transduction Efficiency
AAV2-S261V	~10-fold lower	-*
AAV2-S264V	No change	-*
AAV2-S267V	No DNase I- resistant particles	-*
AAV2-S276V	~10-fold lower	-*
AAV2-S384V	~3-fold higher	~10-fold lower
AAV2-S458V	No change	~4-fold higher
AAV2-S468V	~5-fold higher	No change
AAV2-S492V	No change	~2-fold higher
AAV2-S498V	No change	~10-fold lower
AAV2-S578V	No change	~10-fold lower
AAV2-S658V	~10-fold lower	-*
AAV2-S662V	No change	~20-fold higher
AAV2-S668V	No DNase I-resistant particles	-*
AAV2-S707V	No change	~10-fold lower
AAV2-S721V	No change	No change

Vector packaging and infectivity assays were performed at least twice for each of the mutant-AAV vectors. The packaging efficiency was determined by quantitative PCR analyses. The transduction efficiency was estimated by fluorescence intensity of HEK293 cells infected with an MOI of 1000 vgs/cell.

\* No fluorescence was detected at the MOI tested.

**Table 2**  
**Packaging and transduction efficiencies of serine-mutant vectors replaced with various amino acids relative to WT AAV2 vectors**

Mutant	Packaging Efficiency	Transduction Efficiency
AAV2-S662V	No change	~20-fold higher
AAV2-S662A	~5-fold higher	~3-fold higher
AAV2-S662D	No change	~8-fold higher
AAV2-S662F	~10-fold lower	No change
AAV2-S662H	No change	~4-fold higher
AAV2-S662N	~10-fold lower	No change
AAV2-S662L	~10-fold lower	No change
AAV2-S662I	~10-fold lower	No change

The packaging and infectivity assays were performed as described under the legend to Table 1.

V = Valine; A = Alanine; D = Aspartic acid; F = Phenylalanine H = Histidine; N = Asparagine; L = Leucine; and I = Isoleucine.